Activation of oncogenic pathways in classical Hodgkin lymphoma by decitabine: A rationale for combination with small molecular weight inhibitors

TATJANA MARIA SWEREV, THOMAS WIRTH and ALEXEY USHMOROV

Institute of Physiological Chemistry, University of Ulm, D-89081 Ulm, Germany

Abstract. DNA methylation is an epigenetic control mechanism that contributes to the specific phenotype and to the oncogenic program of virtually all tumor entities. Although efficacy of demethylating agents in classical Hodgkin lymphoma (cHL) was not specifically tested, a case of regression of relapsed metastatic cHL was described as a fortunate side-effect of the demethylating agent 5-azacytidine in a patient with myelodysplastic syndrome. We investigated molecular mechanisms of decitabine (5-Aza-dC) antitumor activity in cHL using gene expression profiling followed by gene set enrichment analysis. We found that 5-Aza-dC inhibits growth of cHL cell lines at clinically relevant concentrations of 0.25-2 μM. The antitumor effect of 5-Aza-dC was associated with induction of genes, which negatively regulate cell cycle progression (e.g. *CDKN1A* and *GADD45A*). Surprisingly, we also observed significant enrichment of pro-survival pathways like MEK/ERK, JAK-STAT and NF-κB, as well as signatures comprising transcription-activating genes. Among the upregulated pro-survival genes were the anti-apoptotic genes *BCL2* and *BCL2L1*, as well as genes involved in transduction of growth and survival signals like *STAT1*, *TLR7*, *CD40* and *IL-6*. We therefore analyzed whether interference with these pro-survival pathways and genes would potentiate the antitumor effect of 5-Aza-dC. We could show that the BCL2/BCL2L1 inhibitor ABT263, the JAK-STAT inhibitors fedratinib and SH-4-54, the AKT inhibitor KP372-1, the NF-κB inhibitor QNZ, as well as the bromodomain and extraterminal (BET) family proteins inhibitor JQ1 acted synergistically with 5-Aza-dC. We conclude that targeting of oncogenic pathways of cHL may improve efficacy of DNA-demethylating therapy in cHL.

Correspondence to: Dr Alexey Ushmorov, Institute of Physiological Chemistry, University of Ulm, Albert-Einstein-Allee 11, D-89081 Ulm, Germany
E-mail: alexey.ushmorov@uni-ulm.de

Introduction

Classical Hodgkin lymphoma (cHL) predominantly is a B-cell malignancy with unique features. Only ~1-5% of the whole tumor mass is represented by Hodgkin and Reed Sternberg (HRS) cells, the malignant component of cHL. The major part of the tumor mass is composed of an inflammatory infiltrate that provides a protective and supportive microenvironment for the tumor cells (1). Despite the 5 year overall survival of 81%, cured patients often suffer from treatment-related complications like pulmonary fibrosis, sterility, and cardiovascular disorders (2). Moreover, they may develop secondary tumors such as acute leukemia and myelodysplastic syndrome (MDS) (2). Thus, a substantial percentage of treatment failures and the high frequency of adverse effects of the chemotherapy warrants the search for novel therapeutic approaches.

Although the HRS cells are derived from germinal or post germinal center B-cells, they have lost most of their B-cell phenotype and express surface markers of various other lineages of the immune system (3). We and others have shown that epigenetic silencing contributes to the extinguishing of the B-cell program in cHL (4-6). In particular, promoter CpG island hyper-methylation was identified as a major cause of silencing of PU.1/SPI1, BOB.1/OBF.1/POU2AF1 and other important regulators of the B-cell program (6). Of note, PU.1 has been shown to act as a tumor suppressor in cHL (7). Additionally, known tumor suppressor genes like p16 and p18INK4c are also epigenetically silenced in cHL (5,7-10).

Epigenetic processes are known to contribute to the oncogenic program in virtually all tumor types by activation of proto-oncogenes or by silencing of tumor suppressor genes (11,12). Unlike the genomic aberrations, epigenetic modifications including CpG dinucleotide methylation and histone deacetylation are reversible by inhibitors of DNA methylation and of histone deacetylases (HDAC), respectively. Currently, the constantly growing list of epigenetic modifiers makes epigenetic therapy one of the most quickly emerging branches of targeted cancer therapy. For some tumors epigenetic therapy is already established as an efficient and less harmful than classical chemotherapy approach to cancer treatment (13). HDAC inhibitors were successfully studied for treatment of cHL. Combination of the pan-HDAC inhibitor

vorinostat with mammalian target of rapamycin (mTOR) inhibitor sirolimus induced complete regression of primary refractory cHL (14). Another pan-HDAC inhibitor panobinostat reduced tumor mass in 74% of patients with relapsed cHL including 23% partial and 4% complete remission (15). HDAC inhibitor entinostat (SNDX-275) has been shown to induce apoptosis in cHL cell lines and entered clinical trials (16).

The DNA methyltransferase (DNMT) inhibitors, in particular decitabine (5-aza-2'-deoxycytidine/5-Aza-dC), is used for treatment of acute myeloid leukemia (AML) (17) and is already approved for treatment of patients with MDS (18). To our knowledge DNMT inhibitors are not specifically tested for use in patients with cHL. However, complete regression of relapsed metastatic cHL was described as a fortunate side-effect in a MDS patient treated with the 5-Aza-dC related demethylating agent 5-azacytidine (19). Both inhibitors have similar function and demonstrated similar efficacy against MDS and AML (20). 5-Aza-dC has often been used by us and others to demonstrate epigenetic mechanisms of gene silencing in cHL cell lines, but assessment of its cytotoxic effects was neglected (4,6,21).

In this study we focused on the possible mechanisms of the antitumor effect of demethylating agents in cHL. Using GEP we could show that along with the reactivation of tumor suppressor genes 5-Aza-dC also induced several oncogenic pathways such as MEK/ERK, JAK-STAT and NF-κB. Here we demonstrate that pharmacological inactivation of some of these pro-survival pathways significantly increases the antitumor effect of 5-Aza-dC against cHL.

Materials and methods

Antibodies and inhibitors. The primary monoclonal mouse antibodies against BCL2 (#sc-509) and ACTB (#sc-130300), as well as the primary polyclonal rabbit antibody against p65 (#sc-372), and the secondary goat anti-rabbit (#sc-2004) and anti-mouse (#sc-2005) antibodies were purchased from Santa Cruz Biotechnology, Inc. (Dallas, TX, USA). The primary monoclonal mouse antibodies against CDKN1A (#556431) and GAGE (#611746) were acquired from BD Bioscience (Heidelberg, Germany). The primary monoclonal rabbit antibodies against BCL2L1 (#2764), and p44/42 MAPK (ERK1/2) (#4695), as well as the primary polyclonal rabbit antibody against phospho-p44/42 MAPK (pERK1/2) (#9101) were purchased from Cell Signaling Technology (Leiden, The Netherlands). The primary monoclonal mouse anti-SSX antibody (#OP196) was acquired from Oncogene Research Products (Boston, MA, USA) and the primary polyclonal rabbit anti-TUBB antibody (#ab6046) from Abcam (Cambridge, UK).

JQ1 was kindly provided by J.E. Bradner (Division of Hematologic Neoplasia, Dana-Faber Cancer Institute, Boston, MA, USA). 5-aza-2'-deoxycytidine (5-Aza-dC) was purchased from Calbiochem (Darmstadt, Germany) and KP372-1 from MoBiTec GmbH (Göttingen, Germany). ABT263, fedratinib, QNZ (EVP4593) and SH-4-54 were acquired from Selleckchem (Munich, Germany). UO126 was purchased from Cell Signaling Technology.

Cell lines and short tandem repeat (STR) analysis. The cHL cell lines L428, and L1236 were cultured in complete RPMI-1640 medium as described earlier (6). The cell lines were obtained from DSMZ (Braunschweig, Germany). The authenticity of the cell lines was proved by STR DNA typing using GenomeLab GeXP™ Genetic Analysis System (Sciex, Darmstadt, Germany) and GenomeLabHuman STR primer set (Beckman Coulter, Krefeld, Germany) as described in user's manual. The obtained STR profiles were compared with comprehensive DSMZ database of STR cell line profiles using 'Online STR Analysis' (www.dsmz.de, 13.08.2015). 5-Aza-dC, if not mentioned differently, was used at a concentration of 1 μM. The cells were seeded at a density of 0.5x10^6/ml and incubated with 5-Aza-dC for 24 h mimicking clinical relevant bolus dose and time schedule. After complete exchange of medium the cells were incubated for another 3 days before harvesting. The cells were counted by a haemocytometer.

Gene expression profiling (GEP). L428, and L1236 cell lines were seeded at a density of 0.5x10^6/ml and incubated with 5-Aza-dC at a concentration of 1 μM for 24 h mimicking clinical relevant bolus dose and time schedule. After complete change of medium the cells were incubated for another 3 days before harvesting. Isolation of the RNA was performed using the RNeasy mini kit (Qiagen, Hilden, Germany) according to the user's manual. Two biological replicates were analyzed for each cell line. Labeling of RNA (cRNA synthesis) was performed by The Microarray Facility, University of Tübingen (Tübingen, Germany) according to a standard Affymetrix® procedure (One-Cycle Target Labeling kit; Affymetrix UK Ltd., High Wycombe, UK). The biotinylated complementary RNA (cRNA) was cleaned and fragmented by a 35 min incubation at 95°C. GeneChip® Human genome U133 Plus 2.0 array (spotted with 1,300,000 oligonucleotides informative for 47,000 transcripts originated from 39,000 genes, Affymetrix UK Ltd.) was used as described in user's manual. We used GeneSifter software for data processing and analysis (www.genesifter.net; 28.09.2015; PerkinElmer, Waltham, MA, USA). Global background correction, across array normalization, and log$_2$ transformation of PM values were done by robust multi-array average (RMA) method. The 3623 probe sets, modulated by 5-Aza-dC at least >3-fold in one of the cell lines, were filtered (threshold X3, Benjamini and Hochberg correction, adjusted P<0.05). The microarray data were deposited in the Gene Expression Omnibus (GEO) database under accession number GSE86068.

Gene set enrichment analysis (GSEA). We used the Broad Institute's Molecular Signatures Database gene set collections 'C2-curated gene sets', and 'C6-oncogenic signatures' for GSEA (http://www.broadinstitute.org/gsea/index.jsp, 02.10.2015) (22,23).

Immunoblot. Cells (1x10^6) were lysed in 100 μl Laemmli buffer containing 6 M urea. Then 25 μl of the protein extracts were separated on 10% polyacrylamide gels by SDS page using the Mini-PROTEAN® Tetra Vertical Electrophoresis (Bio-Rad Laboratories, Munich, Germany) and blotted to a nitrocellulose membrane using the Mini-Electrophoretic Blotting system (CBS Scientific, Del Mar, CA, USA). The membranes were blocked with 5% dry milk in PBS and then incubated with the primary antibodies at 4°C overnight. After several washing steps the membranes were incubated for 1 h with the secondary antibody. Signals were detected with
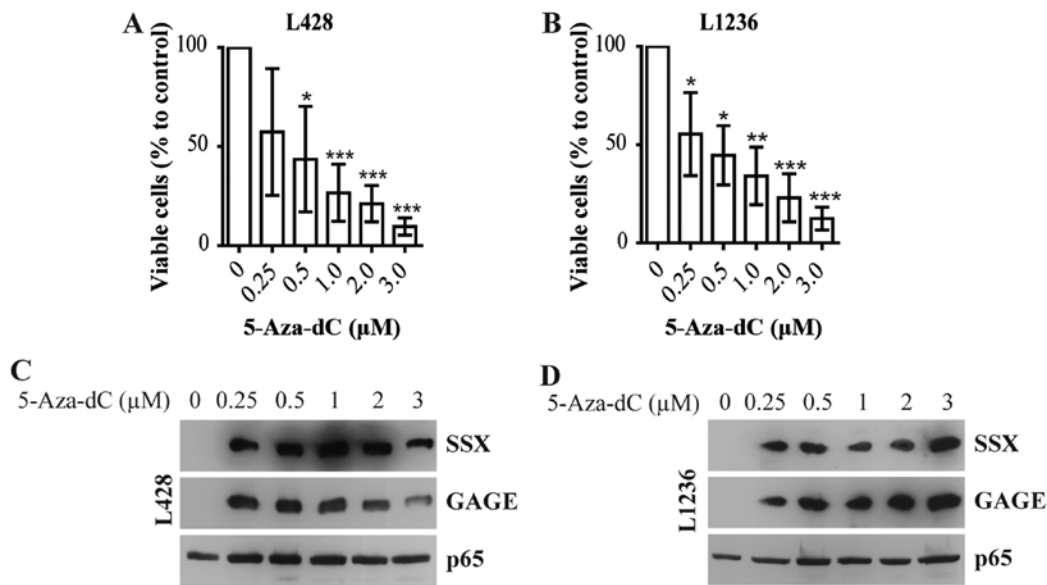
Figure 1. Antitumor effect of 5-Aza-dC and reactivation of cancer/testis antigens. (A and B) 5-Aza-dC *in vitro* treatment protocol mimicking clinical administration scheme is toxic for cHL cell lines. The L428 (A) and L1236 (B) cells were treated with indicated concentrations of 5-Aza-dC for 24 h. After replacement of the medium the cells were incubated for 6 days. The viable cells were counted by haemocytometer using the trypan blue exclusion method. The number of control cells was converted to 100%, whereas the other bars show the relative reduction in cell number after treatment. Results are shown as mean ± SD of three independent experiments. [*]P<0.05, [**]P<0.01 and [***]P<0.001 by the unpaired two-tailed t-test (control vs. treatment). (C and D) 5-Aza-dC effectively demethylates DNA and reactivates epigenetically silenced genes in L428 (C) and L1236 (D) cells. Representative immunoblot detecting the cancer/testis antigens SSX and GAGE after treatment with indicated concentrations of 5-Aza-dC. p65 (RELA) was used as a loading control. The experiment was repeated twice.

the Super Signal West Dura Extended Duration Substrate (Thermo Scientific, Rockford, IL, USA). The representative immunoblots were quantified with help of ImageJ software (imagej.net; 14.01.2016).

Cell viability assay. For measurement of cell viability 50 μl medium containing decreasing concentrations of the specific inhibitors were pipetted in triplicate into flat bottomed 96-well plates creating serial dilutions. Cells/well (2×10^4) were seeded and cultured for 6 days. Then 25 μl 3-(4,5-dimethylthi-azol-2-yl)-2,5-diphenyltetrazolium bromide (MTT) solution from Sigma-Aldrich (Darmstadt, Germany) (5 mg/ml in PBS) per well were added and incubated for 2 h. After dissolving the formazan crystals with MTT-lysis-buffer the absorbance was detected with the Microplate Reader SpectraMax 190 (Molecular Devices, Biberach, Germany) at a wavelength of 570 nm. All experiments were repeated at least two times. The IC_{50} values were generated by using the software CompuSyn (http://www.combosyn.com/, 16.03.2016) with IC_{50} being the concentration where 50% of the maximum possible inhibition was reached (24,25).

Combination plot. 5-Aza-dC was combined with the different inhibitors using decreasing concentrations of the two drugs at a ratio of IC_{50} (5-Aza-dC)/IC_{50} (inhibitor). The drugs were added simultaneously to the cells. The experiment was performed as described in 'Cell viability assay'. The data were analyzed applying the combination index (CI) theorem and plot of Chou and Talalay (24,25) using the CompuSyn software (http://www.combosyn.com/16.03.2016).

Dual luciferase reporter assay and electrophoretic mobility shift assay (EMSA). Nuclear extraction and EMSA were

performed as described earlier (26). The experiment was performed twice. For the reporter assay 1×10^7 cells were transfected by electroporation with the reporter vectors containing binding sides either for STAT3 (Panomics; Gentaur Molecular Products, Aachen, Germany), STAT6 (27) or NF-κB (28) using the Bio-Rad GenePulser II (Bio-Rad Laboratories). The luciferase activity was normalized by cotransfection of the ubi-*Renilla* vector. After 24 h of incubation the luciferase activity was measured with help of the Dual Luciferase Reporter assay system (Promega, Mannheim, Germany) using a luminometer (Berthold Technologies, Bad Wildbach, Germany). This experiment was performed in duplicate and repeated three times.

Statistical analysis. The values of the Dual Luciferase reporter assay and the measurement of cell number are shown as means ± SD. For the statistical analysis the unpaired two-tailed Student's t-test was used. P<0.05 were considered statistically significant. The data were analyzed with help of GraphPad Prism 5 (GraphPad Software, San Diego, CA, USA).

Results

5-Aza-dC is toxic for cHL cell lines and reactivates epigenetically silenced genes at clinically achievable concentrations. In the present study we used a 5-Aza-dC incubation schedule aimed to obtain optimal reactivation of epigenetically silenced genes as we described earlier for cHL (6) and for Burkitt lymphoma (28). Maximal demethylation induced by 5-Aza-dC is achieved after 72 h (29). We incubated the cells for only 24 h with 5-Aza-dC and after complete change of the medium incubated the cells for additional 72 h without drug, to minimize direct toxicity. Using this experimental setting, 5-Aza-dC strongly reduced cell numbers of L428 (Fig. 1A)

Table I. Selected significantly correlated gene sets out of the Curated Gene Sets (C2) and Oncogenic signatures (C6) gene set collections.

Gene sets	NES	NOM P-value	FDR
C2 - Curated Gene Sets			
MIKKELSEN_MEF_HCP_WITH H3_UNMETHYLATED	2.34	0.00	0.00
REACTOME_RNA_POL_I_PROMOTER_OPENING	2.14	0.00	0.00
REACTOME_RNA_POL_I_TRANSCRIPTION	2.09	0.00	0.00
REACTOME_MEIOSIS	2.05	0.00	0.00
KIM_RESPONSE_TO_TSA_AND_DECITABINE_UP	2.03	0.00	0.00
REACTOME_TRANSCRIPTION	2.00	0.00	0.00
C6 - Oncogenic signature			
KRAS.KIDNEY_UP.V1_DN	1.94	0.00	0.02
P53_DN.V1_UP	1.79	0.00	0.11
BRCA1_DN.V1_UP	1.73	0.00	0.18
RELA_DN.V1_DN	1.64	0.01	0.24

NES, normalized enrichment scores; NOM P-value, nominal P-values; FDR, false discovery rates of the selected gene sets.

Table II. Significantly enriched pathways of the Kyoto Encyclopedia of Genes and Genomes (KEGG) pathway enrichment analysis.

KEGG pathway	List	Gene Set	Z-score
Cytokine-cytokine receptor interaction	55	264	5.18
JAK-STAT signaling pathway	32	153	3.93
Toll-like receptor signaling pathway	21	101	3.14
Cell adhesion molecules (CAMs)	24	126	2.89
NOD-like receptor signaling pathway	15	60	2.31
Chemokine signaling pathway	29	182	2.13

and L1236 (Fig. 1B) cHL cell lines. Even concentrations 4-5-fold lower than peak plasma concentration in patients [0.93-2.01 μM (30)] showed significant antitumor effects.

To control the efficacy of the demethylating activity of 5-Aza-dC we analyzed the expression of cancer/testis (CT) antigens SSX and GAGE, a class of genes epigenetically silenced by promoter hypermethylation in differentiated cells, which can be reactivated by 5-Aza-dC in cHL cell lines (31). 5-Aza-dC induced expression of SSX and GAGE in L428 (Fig. 1C) and L1236 (Fig. 1D) cell lines at all concentrations used.

Thus, 5-Aza-dC shows antitumor effects against cHL cell lines when used at clinically relevant concentrations.

5-Aza-dC activates main oncogenic pathways of cHL. To characterize the molecular mechanisms involved in the 5-Aza-dC antitumor effect, we used GEP. With help of Genesifter software we filtered out 3623 probe sets modulated more than 3-fold in at least one of the two cell lines. To identify modulated pathways we first used Gene Set Enrichment Analysis (GSEA) (Table I). Among the significantly enriched signatures (FDR<0.25; nominal P<0.05) were P53_DN.V1_UP (Fig. 2A and Table I),

comprising 194 genes upregulated in cell lines with mutated TP53, KRAS.KIDNEY_UP.V1_DN (Fig. 2B and Table I), containing 142 genes induced in epithelial kidney cancer cells by overexpression of KRAS, and RELA_DN.V1_DN (Fig. 2C and Table I), consisting of 141 genes upregulated in kidney fibroblasts with mutated RELA. Applying the utility 'Gene function' of the Genesifter software we showed that among the genes of the TP53 signature *X57348* (SFN), a TP53 stabilizer and a negative regulator of cell cycling, was on top of the list (Fig. 3A) (32). The TP53 associated gene list also included *CDKN1A*, *GADD45A* and *GADD45B*, as well as apoptosis-associated TP53 target gene *TP53I3* (Fig. 3A) (33). Another potential tumor suppressor gene in TP53 annotation was thrombospondin 1 (*THBS1*), that facilitates RAS-induced senescence by repressing ERK signaling (Fig. 3A) (34). Surprisingly, among the upregulated genes we also found repression targets of TP53 including genes that support cell cycle progression (*CCND1*, *CCND2* and *CDK6*). Among the upregulated genes of KRAS signature were also the positive regulator of transcription *BRDT* (35) and protooncogene *SRC*. Moreover, we found that signatures of the gene sets REACTOME_TRANSCRIPTION (Fig. 2D and Table I) and MIKKELSEN_MEF_WITH_H3_UNMETHYLATED (Fig. 2E and Table I) were significantly enriched, suggesting that 5-Aza-dC not only demethylates epigenetically silenced genes, but raises global transcription levels in cHL cell lines.

We further applied Kyoto Encyclopedia of Genes and Genomes (KEGG) database analysis to identify additional significantly upregulated signatures (Table II). Two of the pathways with highest enrichment scores were 'JAK-STAT signaling pathway' (z-score, 3.93) (Fig. 3B and Table II), and 'Cytokine-cytokine receptor interaction' (z-score, 5.18) (Fig. 3C and Table II). Among upregulated genes of 'Cytokine-cytokine receptor interaction' signature were *CXCL10*, *IL-6*, *IL-6R* and *IL-13*, that provide growth and survival signals to the HRS cells (Fig. 3C) (36,37). In addition, among the upregulated genes of JAK-STAT signature were positive regulators of cell cycling *CCND1* and *CCND2* and
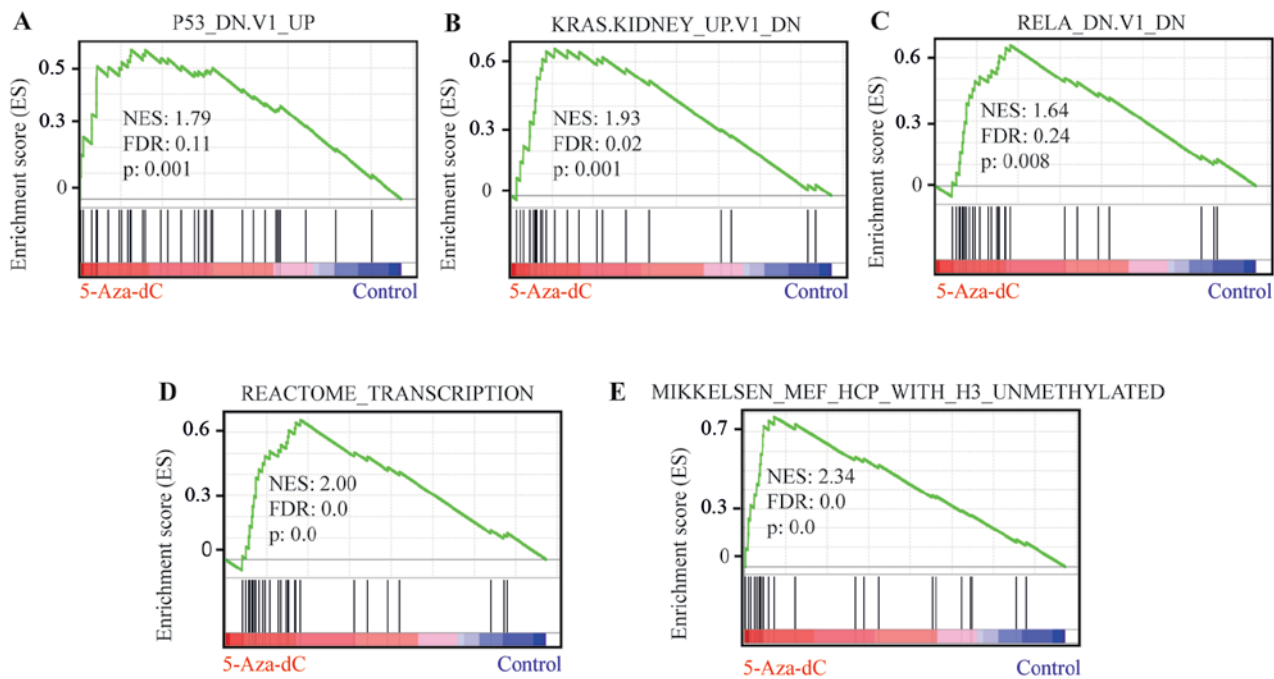
Figure 2. Activation of pro-survival pathways by 5-Aza-dC. (A-E) The microarray data were analyzed with Gene Set Enrichment Analysis (GSEA) choosing C2 (curated gene sets) and C6 (oncogenic signatures) as gene set collections out of the Broad Institute's Molecular Signatures Database. The analysis is based on the calculation of an enrichment score (green line) which increases with higher correlation between the chosen gene sets and the microarray data. (A) Enrichment plot of the gene set P53_DN.V1_UP. (B) Enrichment plot of the gene set KRAS.KIDNEY_UP.V1_DN. (C) Enrichment plot of the gene set RELA_DN.V1_DN. (D) Enrichment plot of the gene set REACTOME_ TRANSCRIPTION. (E) Enrichment plot of the gene set MIKKELSEN_MEF_HCP_ WITH_H3_UNMETHYLATED.

critical for cHL survival anti-apoptotic gene *BCL2L1* (Fig. 3B). The NF-κB target gene *STAT5A*, which is constitutively active in cHL (38), was upregulated as well (Fig. 3B). Then we applied the utility 'Gene function' of the Genesifter software to identify other pro-survival genes using the ontologies 'ERK1 and ERK2 cascade' (Fig. 3D), 'NF-κB/IκB signaling' (Fig. 3E) and 'negative regulation of apoptosis' (Fig. 3F). This helped us to identify several other important upregulated proto-oncogenes including *BCL2*.

We suggested that, although 5-Aza-dC has antitumor effect in cHL cell lines, it may be hampered by activation of pro-survival pathways including JAK-STAT, NF-κB and KRAS.

Validation of GEP results. To validate results of the GEP we measured the expression of selected genes by immunoblot. We found that 5-Aza-dC strongly induced CDKN1A protein synthesis at a broad range of concentrations (Fig. 4A and B). One of the main functions of CDKN1A is the inhibition of CDK2, which is among other proteins responsible for cell cycle progression through S phase (39). Moreover, CDKN1A is an antiapoptotic protein that induces cell cycle arrest and downregulates pro-apoptotic genes such as procaspase-3 or caspase-8 (39). We also proved the upregulation of the antiapoptotic proteins BCL2 (Fig. 4C and D) and BCL2L1 (Fig. 4C and E).

5-Aza-dC activates MEK/ERK signaling. Since GEP and subsequent enrichment analysis indicated induction of critical oncogenic pathways in cHL, we assessed activity of MEK/ERK, JAK-STAT and NF-κB pathways. We first assessed the phosphorylation status of ERK1/2 using immunoblot. 5-Aza-dC

strongly induced the phosphorylation of ERK1 in one the two cell lines and phosphorylation of ERK2 in both cell lines with no changes seen in the levels of unphosphorylated ERK1/2 protein expression (Fig. 5A). Next using EMSA we investigated NF-κB pathway activation. No significant increase but rather decrease of NF-κB binding could be detected in treated cells compared to control cells in both cell lines (Fig. 5B). In addition we analyzed NF-κB activation by 5-Aza-dC in L428 cells with help of luciferase reporter assay using a vector containing three κB binding sites. The luciferase reporter assay did also not reveal induction of NF-κB-dependent transcription (Fig. 5C). Finally we analyzed the activity of the JAK-STAT pathway in L428 cells using luciferase-expression vectors harboring STAT3 (Fig. 5D) and STAT6 (Fig. 5E) promoters. We did not see an increase of luciferase activity in L428 cells after treatment with 5-Aza-dC.

Thus, although 5-Aza-dC significantly enriched gene expression signatures of main oncogenic pathways of cHL, it did not directly facilitate nuclear translocation of STATs and NF-κB. This implies that other mechanisms, like transcription-activating chromatin modifications of STAT and NF-κB target genes, may contribute to the 5-Aza-dC induced activation of these pathways.

Inhibition of the upregulated oncogenic pathways increases the antitumor effect of 5-Aza-dC. We assumed that targeting of the activated pro-survival pathways may potentiate the antitumor effect of 5-Aza-dC. Given that 5-Aza-dC also induced genes activating transcription, we also included the BET inhibitor JQ1 which blocks transcriptional activation through interaction with acetylated chromatin.
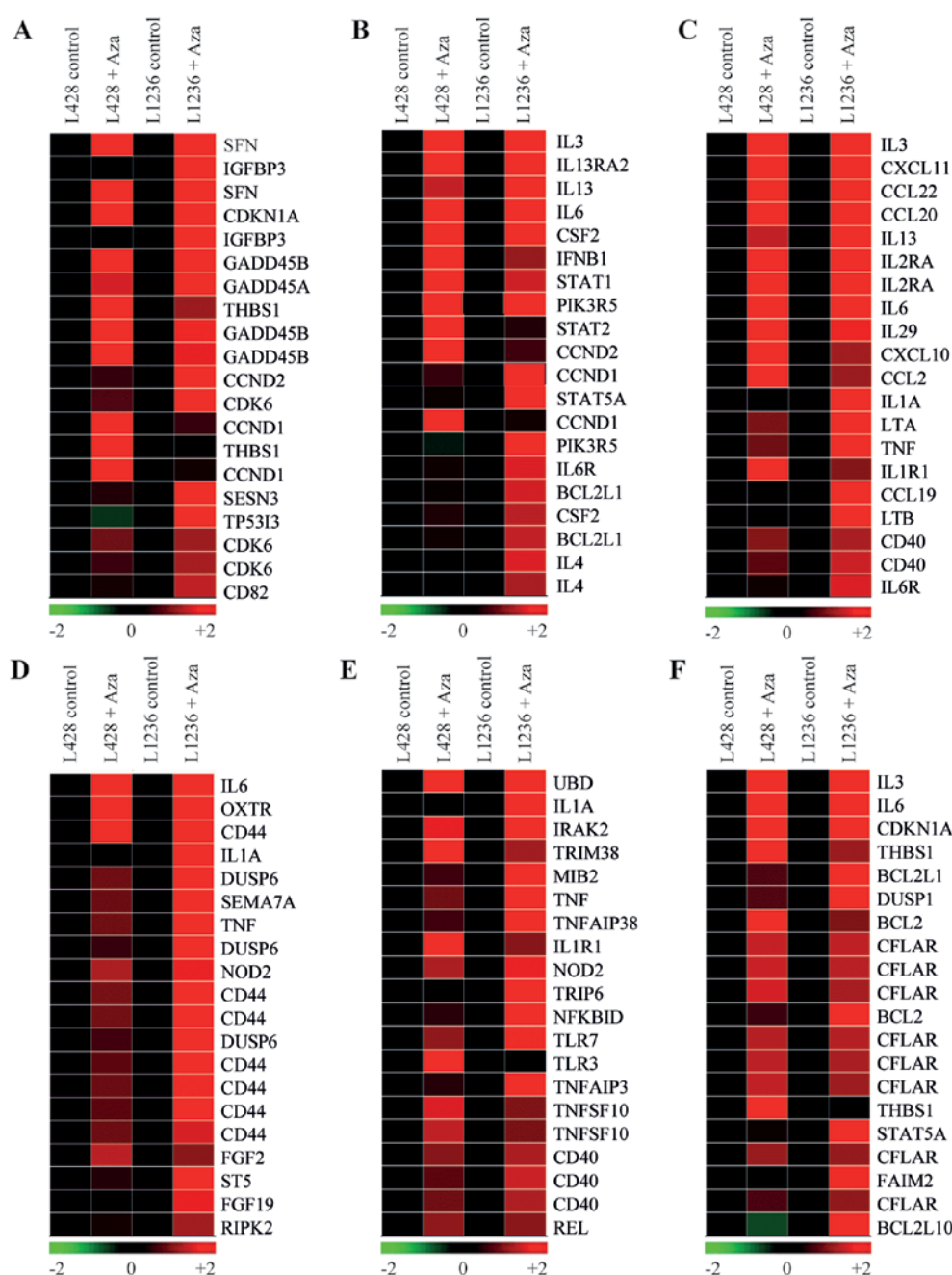
Figure 3. Enrichment analysis of GEP data. (A-F) Heatmaps of the enriched pathways. Upregulation is shown by color coding in a log₂ scale. All genes are sorted by expression with the highest upregulated genes on the top. (A) Twenty selected upregulated genes belonging to p53 signaling pathway. (B) Twenty selected upregulated genes of the Kyoto Encyclopedia of Genes and Genomes (KEGG) pathway 'JAK-STAT-signaling pathway'. (C) Twenty selected upregulated genes of the KEGG pathway 'Cytokine-cytokine receptor interaction'. (D) Twenty selected upregulated genes of 'ERK1 and ERK2 cascade'. (E) Twenty selected upregulated genes of 'NF-κB/IκB signaling'. (F) Twenty selected upregulated genes of 'negative regulation of apoptosis'.

First we assessed the antitumor effects of the single treatments by calculating their IC$_{50}$ values (Tables III and IV). L428 and L1236 showed different sensitivity to the inhibitors. The BCL2/BCL2L1 inhibitor ABT263 had the highest cytotoxic activity in both cell lines (Tables III and IV). The least toxic were the MEK inhibitor UO126, and the STAT3/STAT5 inhibitor SH-4-54, although UO126 had somehow stronger activity in L1236 and SH-4-54 in L428 cell lines (Tables III and IV). The JAK inhibitor fedratinib had strong antitumor activity against L1236, whereas L428 cells were less sensitive (Tables III and IV). The NF-κB pathway inhibitor QNZ, AKT inhibitor KP372-1, the bromodomain

and extra-terminal (BET) family proteins inhibitor JQ1 also differed in their antitumor effect towards cHL cell lines. L428 was more sensitive to KP372-1 and QNZ (Table III), whereas JQ1 showed a stronger antitumor effect in L1236 (Table IV).

To analyze the dose effect relationships of the drug combinations we applied the method of Chou and Talaly (24,25). With help of the CompuSyn Software we produced CI-Fa combination plots. The CI represents the value of the effect of the combined drugs, with CI values >1 indicating antagonism, CI values =1 additive effects, and CI values <1 synergism (24,25). The fraction affected (Fa) values represent the magnitude of the antitumor effect of the combination.

Table III. Results of IC_{50} calculation and combination plot in L428.

Cell line L428 Drugs	Parameters			CI values		
	IC_{50} (nM)	m	r	ED_{35}	ED_{50}	ED_{90}
Aza	57.2	0.89	0.96			
Fedratinib	710.5	3.06	0.97			
Fedratinib + Aza (12.4:1)	217.7	1.37	1.00	0.58	0.57	0.80
Aza	57.2	0.89	0.96			
JQ1	182.4	0.23	0.41			
JQ1 + Aza (3.2:1)	24.6	0.83	0.97	0.84	0.21	0.12
Aza	57.2	0.89	0.96			
KP372-1	346.7	3.46	0.98			
KP372-1 + Aza (6.1:1)	168.7	2.28	0.93	1.02	0.83	0.67
Aza	57.2	0.89	0.96			
QNZ	143.6	1.07	1.00			
QNZ+ Aza (2.5:1)	17.15	2.71	0.88	0.14	0.07	0.01
Aza	57.2	0.89	0.96			
SH-4-54	3925.3	7.62	1.00			
SH-4-54 + Aza (68.6:1)	1402.9	2.81	0.94	0.88	0.71	0.64
Aza	57.2	0.89	0.96			
UO126	5734.0	1.99	0.98			
UO126 + Aza (100.2:1)	2753.6	0.74	0.95	282.27	475.96	3043.62
Aza	57.2	0.89	0.96			
ABT263	14.8	1.34	0.99			
ABT263 + Aza (1:3.9)	23.4	1.05	0.98	0.65	0.65	0.75

The L428 cells were incubated for 6 days with the single drugs or the indicated combinations of the inhibitors. Cell viability was measured using MTT assay. IC_{50} is presented in nM and represents the concentration where 50% of the maximum possible inhibition is reached. m, represents the shape of the dose-effect curves with m>1 indicating sigmoid, m=1 hyperbolic and m<1 flat sigmoid curves (24). r, represents the linear correlation coefficient of the median effect plot (24). CI value at EDx represents the Combination Index when x% of the maximum possible inhibition is achieved with CI values >1 indicate antagonism, CI values =1 additive effects and CI values <1 synergism (24).
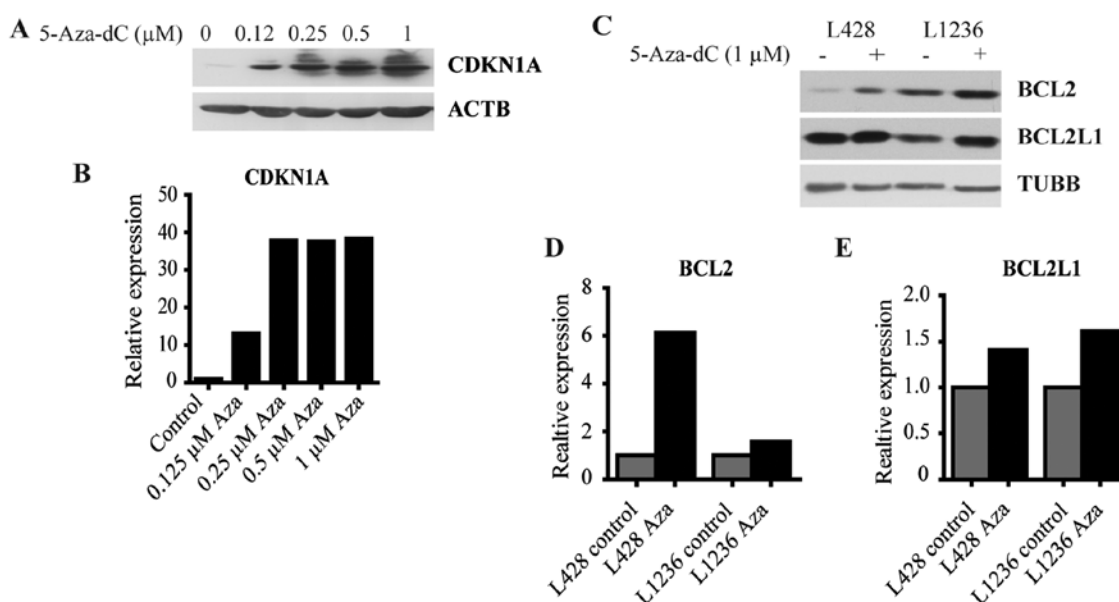

Figure 4. Validation of selected upregulated genes in the GEP by immunoblot. (A) Upregulation of cyclin-dependent kinase inhibitor CDKN1A after treatment with increasing concentrations of 5-Aza-dC (Aza). ACTB was used as a loading control. (B) Relative quantification of the CDKN1A protein concentration by ImageJ software. (C) Representative immunoblot detecting the antiapoptotic proteins BCL2 and BCL2L1 after treatment with 1 μM 5-Aza-dC. Tubulin B (TUBB) was used as a loading control. (D and E) Relative quantification of representative BCL2 (D) and BCL2L1 (E) immunoblots by ImageJ software. The experiments were performed three times.

Table IV. Results of IC_{50} calculation and combination plot in L1236.

Cell line L1236	Parameters			CI values		
Drugs	IC_{50} (nM)	m	r	ED_{35}	ED_{50}	ED_{90}
Aza	1956.8	0.84	0.99			
Fedratinib	81.1	1.03	0.99			
Fedratinib + Aza (1:24.1)	2141.5	0.87	1.00	2.01	2.10	2.57
Aza	1956.8	0.84	0.99			
JQ1	47.8	1.42	0.98			
JQ1 + Aza (1:41.0)	1557.2	0.80	0.96	1.30	1.55	3.46
Aza	1956.8	0.84	0.99			
KP372-1	611.4	1.72	1.0			
KP372-1 + Aza (1:3.2)	991.7	1.30	0.94	0.75	0.77	1.94
Aza	1956.8	0.84	0.99			
QNZ	947.3	0.74	0.95			
QNZ+ Aza (1:2.1)	350.6	0.79	1.00	0.24	0.24	0.24
Aza	1956.8	0.84	0.99			
SH-4-54	5387.3	14.52	1.0			
SH-4-54 + Aza (2.8:1)	4079.3	4.61	0.80	1.52	1.11	0.83
Aza	1956.8	0.84	0.99			
UO126	4430.7	2.62	0.99			
UO126 + Aza (2.3:1)	6930.8	0.63	0.99	1.37	2.17	17.52
Aza	1956.8	0.84	0.99			
ABT263	10.0	1.65	0.99			
ABT263 + Aza (1:196.0)	1381.8	0.61	0.96	0.90	1.40	8.60

The L1236 cells were incubated for 6 days with the single drugs or the indicated combinations of the inhibitors. Cell viability was measured using MTT assay. IC_{50} is presented in nM and represents the concentration where 50% of the maximum possible inhibition is reached. m, represents the shape of the dose-effect curves with m>1 indicating sigmoid, m=1 hyperbolic and m<1 flat sigmoid curves (24). r, represents the linear correlation coefficient of the median effect plot (24). CI value at EDx represents the Combination Index when x% of the maximum possible inhibition is achieved with CI values >1 indicate antagonism, CI values =1 additive effects and CI values <1 synergism (24).
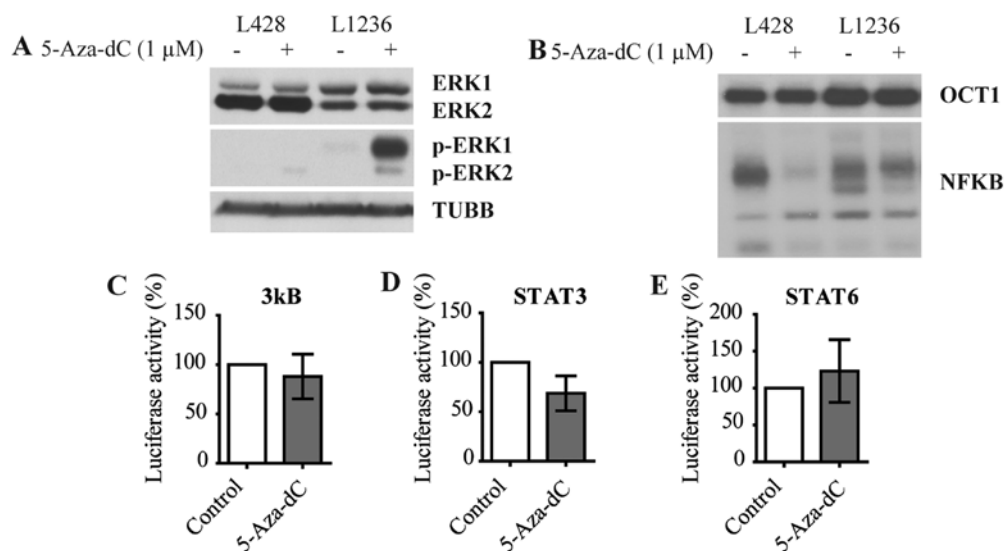

Figure 5. Effect of 5-Aza-dC on ERK, STAT and NF-κB activation status. (A) Phosphorylation status of ERK after treatment with 1 μM 5-Aza-dC was analyzed by immunoblot. Unphosphorylated ERK1/2 and TUBB were used as loading controls. The experiments were done in triplicate. (B) EMSA detecting NF-κB nuclear translocation and binding to DNA. Nuclear extracts were incubated with radio-labeled DNA probes containing binding sites for κB or Oct-1. The labeled probes were separated on a native polyacrylamide gel. The experiment was performed in duplicate with similar results. (C-E) The L428 cells were transfected with reporter vectors containing binding sites for the indicated transcription factors. Luciferase activity was assessed as described in Materials and methods. Relative luciferase activity is presented as mean ± SD of four independent experiments. The luciferase activity of the untreated cells was converted to 100%, whereas the others bars show the relative changes in light emission.
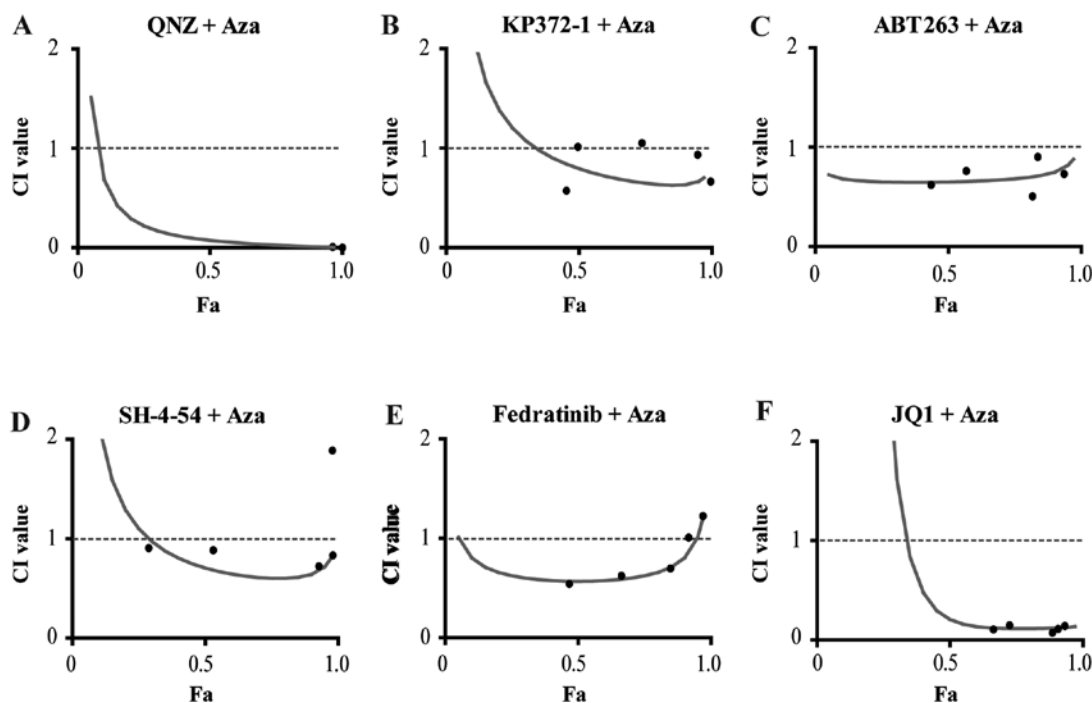
Figure 6. Selective pathway inhibition increases the antitumor effect of 5-Aza-dC in L428 cells. (A-F) Combination of 5-Aza-dC (Aza) with indicated inhibitors showed synergistic effects in L428 cells. The cells were incubated for 6 days with the indicated combinations of the inhibitors. Cell viability was measured using MTT assay. The curves with solid line seen on the fraction affected (Fa), Combination Index (CI) plot represent the predictive values calculated by the CompuSyn software. The dots shown on the plot represent the experimental combination data. CI values >1 indicate antagonism, CI values =1 indicate an additive effect and CI values <1 indicate synergism of the two drugs. The experiments were performed twice. (A) Combination of 5-Aza-dC with the NF-κB pathway inhibitor QNZ. (B) Combination of 5-Aza-dC with the AKT/PDK1 inhibitor KP372-1. (C) Combination of 5-Aza-dC with the BCL2/BCL2L1 inhibitor ABT263. (D) Combination of 5-Aza-dC with the JAK-STAT pathway inhibitors SH-4-54 and (E) fedratinib. (F) Combination of 5-Aza-dC with the BET inhibitor JQ1.

Fa=0 indicates the absence of therapeutic effects, and Fa=1 the maximum achievable antitumor activity (24,25). For each Fa value the software generates a predictive CI value, which can be seen on the plots as the curves with the solid line. The experimental combination data, that were used to generate the CI-Fa combination plots, are represented as dots (24,25).

Similar to the single treatments, cHL cell lines varied in terms of sensitivity to the drug combinations. In general, L428 cells were more sensitive than L1236 cells. The most effective in both cell lines was the combination with the NF-κB inhibitor QNZ (Fig. 6A and Table IV). Targeting AKT, one of the downstream molecules in NF-κB signaling, with the AKT-inhibitor KP372-1, resulted in synergistic antitumor effects in both cell lines (Fig. 6B and Table IV).

Combination of 5-Aza-dC with the BCL2/BCL2L1 inhibitor ABT263 resulted in very strong synergy especially in L428 (Fig. 6C). In L1236 a synergistic effect could only be observed at low Fa values (Table IV). Targeting the JAK-STAT pathway by combining 5-Aza-dC with the STAT3/STAT5 inhibitor SH-4-54 (Fig. 6D) or JAK2 inhibitor fedratinib (Fig. 6E) showed synergistic effects in L428 at almost all concentrations. In L1236 only SH-4-54 showed a slight synergistic effect at intermediate Fa values (Table IV). Fedratinib did not increase the antitumor effect of 5-Aza-dC in L1236 (Table IV).

Among the gene sets significantly enriched by 5-Aza-dC we identified REACTOME_TRANSCRIPTION, that comprises genes involved in transcription. We applied the concept of dual epigenetic therapy to inhibit the 5-Aza-dC-induced

transcription activation. The inhibitor JQ1 inhibits BRDs binding to acetylated histones (35). We observed synergism at high concentration in L428 cells (Fig. 6F) and at low concentrations in L1236 cells (Table IV).

Given the positive effect of 5-Aza-dC on ERK activation we expected to observe strong synergy with MEK inhibitors. Against our expectations, combination with the MEK inhibitor UO126 showed strong antagonistic effects in both cell lines (Tables III and IV).

Thus, inhibition of pro-survival pathways induced by 5-Aza-dC in cHL cell lines potentiates the antitumor effect.

Discussion

Here we provide experimental evidence that the demethylating agent 5-Aza-dC has antitumor effects on cHL. However, the magnitude of the effect is hampered by simultaneous induction of pro-survival pathways. The inhibition of these pathways significantly improved the antitumor activity of 5-Aza-dC.

5-Aza-dC was successfully used for treatment of a wide spectrum of tumors (40). In cHL there is only one anecdotic evidence on clinical efficacy of 5-Aza-dC (19). In addition it was suggested that 5-Aza-dC could be used for increasing immunogenicity of HRS cells and to make them a more attractive target for T-cell therapy (41). This study on antitumor effects of 5-Aza-dC at clinically relevant concentrations supports the idea on the feasibility of demethylating therapy for cHL.

At the same time we revealed a serious drawback of 5-Aza-dC treatment. We detected a significant upregulation

of the pathways, that are known to contribute to the oncogenic program of cHL (MEK/ERK, NF-κB and JAK-STAT) (1). The ability of 5-Aza-dC to modulate MEK/ERK activity is cell type specific and depends on the activation status of other pathways. In ovarian cancer cell lines, 5-Aza-dC strongly activated ERK phosphorylation only in cell lines harboring activating KRAS mutations (42). In the human AML cell line NB4 and in freshly isolated AML cells, 5-Aza-dC also stimulated ERK phosphorylation (43). In other normal and malignant cell types including osteoclasts (44), acute lymphoblastic leukemia (45), and lung cancer cell lines (46) 5-Aza-dC attenuated MEK/ERK activity, *inter alia* by reactivating epigenetically silenced negative regulators. JAK-STAT signaling is inhibited by 5-Aza-dC, in particular by the reactivation of JAK-STAT inhibitors (47,48).

The effect of 5-Aza-dC on NF-κB activity is cell-type dependent. 5-Aza-dC activated NF-κB signaling in Burkitt lymphoma (28) and in AML (49), but inhibited NF-κB activity in osteoclasts (44). Of note, although in our experiments we observed significant upregulation of NF-κB and STAT target genes, this was not mediated by increased nuclear translocation of these transcription factors. Most probably the increasing transcription of NF-κB and STAT targets reflects solely general stimulating effects of 5-Aza-dC on chromatin structure. It was shown that 5-Aza-dC increases global histones acetylation independent of DNA methylation (50). Thus, 5-Aza-dC not only induces activation of hypermethylated promoters but also stimulates transcriptional activity of already active genes, i.e. the genes constituting tumor survival and proliferation programs.

Consequently we have shown that repression of the activated pro-survival pathways can potentiate the antitumor effect of 5-Aza-dC. So far, 5-Aza-dC was used in combination with chemotherapeutics to prevent or reverse epigenetic silencing of genes mediating the cytotoxic effect (51). Combination of 5-Aza-dC with epidermal growth factor receptor inhibitor gefitinib has synergistic antitumor effects against colon carcinoma cells (52).

To potentiate the antitumor effect of 5-Aza-dC on cHL cell lines, we targeted JAK-STAT and NF-κB pathways. As a single treatment the small molecular weight inhibitor of JAK2 fedratinib already showed strong antitumor activity against cHL *in vitro* and *in vivo* (53). Our findings provide a rationale for combination of this inhibitor with 5-Aza-dC. Targeting NF-κB with the inhibitor QNZ also significantly increased the antitumor effect of 5-Aza-dC. Of note, other NF-κB inhibitors like the proteasome inhibitor bortezomib were considered as an attractive approach to treat cHL (54), however clinical trials did not meet the expectations (55). We hope that combination with 5-Aza-dC may be a way to improve the efficacy of NF-κB inhibitors.

We found that MEK/ERK signaling, which is constitutively active in most of the HRS cells (1), was activated by 5-Aza-dC. Unexpectedly, we revealed antagonistic interactions between 5-Aza-dC and MEK1/2 inhibitor U0126. Interestingly, Stewart *et al* described a decrease in the sensitivity of an ovarian cancer cell line to the ERK inhibitor trametinib by treatment with 5-Aza-dC and attributed it to 5-Aza-dC-induced ERK hyper-activation (42). It is conceivable that ERK-dependent induction of BCL2 and BCL2L1 (56) contributed to the protective effect of 5-Aza-dC. Our data on strong synergistic effects of BCL2/BCL2L1 inhibitor

ABT263 with 5-Aza-dC supports this assumption. Synergism of 5-Aza-dC with BCL2 inhibitors was described earlier in ovarian cancer models (42).

We could also observe strong synergism of 5-Aza-dC with the BET inhibitor JQ1. JQ1 predominantly inhibits transcription of oncogenes highly expressed in tumor cells, including MYC, by preventing recruitment of transcription activating BET proteins to acetylated histones (57). Considering a functional connection between histone modifications and DNA methylation it is not surprising that treatment with 5-Aza-dC induces histone acetylation and activation of transcription (50). It is therefore conceivable, that JQ1 blocks this 5-Aza-dC-induced transcriptional activation. Interestingly, the synergistic interaction between JQ1 and hypomethylating drugs has been predicted earlier (58).

Due to its low toxicity 5-Aza-dC is an attractive alternative for classical chemotherapy especially in elderly patients and for palliative care (59). Combination of epigenetic therapy with matched pathway inhibition may therefore be a promising approach to treat elderly and multi-morbid patients with cHL. Further *in vitro* and *in vivo* studies will be required to fully understand the potential of the different combinations and to evaluate their toxicity profile.

References

1. Küppers R: The biology of Hodgkin's lymphoma. Nat Rev Cancer 9: 15-27, 2009.
2. Gobbi PG, Ferreri AJ, Ponzoni M and Levis A: Hodgkin lymphoma. Crit Rev Oncol Hematol 85: 216-237, 2013.
3. Küppers R and Hansmann ML: The Hodgkin and Reed/Sternberg cell. Int J Biochem Cell Biol 37: 511-517, 2005.
4. Doerr JR, Malone CS, Fike FM, Gordon MS, Soghomonian SV, Thomas RK, Tao Q, Murray PG, Diehl V, Teitell MA, *et al*: Patterned CpG methylation of silenced B cell gene promoters in classical Hodgkin lymphoma-derived and primary effusion lymphoma cell lines. J Mol Biol 350: 631-640, 2005.
5. Ehlers A, Oker E, Bentink S, Lenze D, Stein H and Hummel M: Histone acetylation and DNA demethylation of B cells result in a Hodgkin-like phenotype. Leukemia 22: 835-841, 2008.
6. Ushmorov A, Leithäuser F, Sakk O, Weinhäusel A, Popov SW, Möller P and Wirth T: Epigenetic processes play a major role in B-cell-specific gene silencing in classical Hodgkin lymphoma. Blood 107: 2493-2500, 2006.
7. Yuki H, Ueno S, Tatetsu H, Niiro H, Iino T, Endo S, Kawano Y, Komohara Y, Takeya M, Hata H, *et al*: PU.1 is a potent tumor suppressor in classical Hodgkin lymphoma cells. Blood 121: 962-970, 2013.
8. García JF, Villuendas R, Algara P, Sáez AI, Sánchez-Verde L, Martínez-Montero JC, Martínez P and Piris MA: Loss of p16 protein expression associated with methylation of the p16INK4A gene is a frequent finding in Hodgkin's disease. Lab Invest 79: 1453-1459, 1999.

9. Sánchez-Aguilera A, Delgado J, Camacho FI, Sánchez-Beato M, Sánchez L, Montalbán C, Fresno MF, Martín C, Piris MA and García JF: Silencing of the p18INK4c gene by promoter hypermethylation in Reed-Sternberg cells in Hodgkin lymphomas. Blood 103: 2351-2357, 2004.

10. Guan H, Xie L, Leithäuser F, Flossbach L, Möller P, Wirth T and Ushmorov A: KLF4 is a tumor suppressor in B-cell non-Hodgkin lymphoma and in classic Hodgkin lymphoma. Blood 116: 1469-1478, 2010.

11. Pathania R, Ramachandran S, Elangovan S, Padia R, Yang P, Cinghu S, Veeranan-Karmegam R, Arjunan P, Gnana-Prakasam JP, Sadanand F, et al: DNMT1 is essential for mammary and cancer stem cell maintenance and tumorigenesis. Nat Commun 6: 6910, 2015.

12. Völkel P, Dupret B, Le Bourhisxand Angrand PO: Diverse involvement of EZH2 in cancer epigenetics. Am J Transl Res 7: 175-193, 2015.

13. VanderMolen KM, McCulloch W, Pearce CJ and Oberlies NH: Romidepsin (Istodax, NSC 630176, FR901228, FK228, depsipeptide): A natural product recently approved for cutaneous T-cell lymphoma. J Antibiot (Tokyo) 64: 525-531, 2011.

14. Subbiah V, Brown RE, McGuire MF, Buryanek J, Janku F, Younes A and Hong D: A novel immunomodulatory molecularly targeted strategy for refractory Hodgkin's lymphoma. Oncotarget 5: 95-102, 2014.

15. Oki Y, Copeland A and Younes A: Clinical development of panobinostat in classical Hodgkin's lymphoma. Expert Rev Hematol 4: 245-252, 2011.

16. Jóna A, Khaskhely N, Buglio D, Shafer JA, Derenzini E, Bollard CM, Medeiros LJ, Illés A, Ji Y and Younes A: The histone deacetylase inhibitor entinostat (SNDX-275) induces apoptosis in Hodgkin lymphoma cells and synergizes with Bcl-2 family inhibitors. Exp Hematol 39: 1007-1017.e1, 2011.

17. Kim TK, Gore SD and Zeidan AM: Epigenetic therapy in acute myeloid keukemia: Current and future directions. Semin Hematol 52: 172-183, 2015.

18. Saba HI: Decitabine in the treatment of myelodysplastic syndromes. Ther Clin Risk Manag 3: 807-817, 2007.

19. D'Alò F, Leone G, Hohaus S, Teofili L, Bozzoli V, Tisi MC, Rufini V, Calcagni ML and Voso MT: Response to 5-azacytidine in a patient with relapsed Hodgkin lymphoma and a therapy-related myelodysplastic syndrome. Br J Haematol 154: 141-143, 2011.

20. Derissen EJ, Beijnen JH and Schellens JH: Concise drug review: Azacitidine and decitabine. Oncologist 18: 619-624, 2013.

21. Ushmorov A, Ritz O, Hummel M, Leithäuser F, Möller P, Stein H and Wirth T: Epigenetic silencing of the immunoglobulin heavy-chain gene in classical Hodgkin lymphoma-derived cell lines contributes to the loss of immunoglobulin expression. Blood 104: 3326-3334, 2004.

22. Mootha VK, Lindgren CM, Eriksson KF, Subramanian A, Sihag S, Lehar J, Puigserver P, Carlsson E, Ridderstråle M, Laurila E, et al: PGC-1alpha-responsive genes involved in oxidative phosphorylation are coordinately downregulated in human diabetes. Nat Genet 34: 267-273, 2003.

23. Subramanian A, Tamayo P, Mootha VK, Mukherjee S, Ebert BL, Gillette MA, Paulovich A, Pomeroy SL, Golub TR, Lander ES, et al: Gene set enrichment analysis: A knowledge-based approach for interpreting genome-wide expression profiles. Proc Natl Acad Sci USA 102: 15545-15550, 2005.

24. Chou TC: Theoretical basis, experimental design, and computerized simulation of synergism and antagonism in drug combination studies. Pharmacol Rev 58: 621-681, 2006.

25. Chou TC and Talalay P: Quantitative analysis of dose-effect relationships: The combined effects of multiple drugs or enzyme inhibitors. Adv Enzyme Regul 22: 27-55, 1984.

26. Maier HJ, Schips TG, Wietelmann A, Krüger M, Brunner C, Sauter M, Klingel K, Böttger T, Braun T and Wirth T: Cardiomyocyte-specific IκB kinase (IKK)/NF-κB activation induces reversible inflammatory cardiomyopathy and heart failure. Proc Natl Acad Sci USA 109: 11794-11799, 2012.

27. Ritz O, Guiter C, Dorsch K, Dusanter-Fourt I, Wegener S, Jouault H, Gaulard P, Castellano F, Möller P and Leroy K: STAT6 activity is regulated by SOCS-1 and modulates BCL-XL expression in primary mediastinal B-cell lymphoma. Leukemia 22: 2106-2110, 2008.

28. Guan H, Xie L, Klapproth K, Weitzer CD, Wirth T and Ushmorov A: Decitabine represses translocated MYC oncogene in Burkitt lymphoma. J Pathol 229: 775-783, 2013.

29. Bender CM, Gonzalgo ML, Gonzales FA, Nguyen CT, Robertson KD and Jones PA: Roles of cell division and gene transcription in the methylation of CpG islands. Mol Cell Biol 19: 6690-6698, 1999.

30. Atallah E, Kantarjian H and Garcia-Manero G: The role of decitabine in the treatment of myelodysplastic syndromes. Expert Opin Pharmacother 8: 65-73, 2007.

31. Shafer JA, Cruz CR, Leen AM, Ku S, Lu A, Rousseau A, Heslop HE, Rooney CM, Bollard CM and Foster AE: Antigen-specific cytotoxic T lymphocytes can target chemoresistant side-population tumor cells in Hodgkin lymphoma. Leuk Lymphoma 51: 870-880, 2010.

32. Hermeking H and Benzinger A: 14-3-3 proteins in cell cycle regulation. Semin Cancer Biol 16: 183-192, 2006.

33. Polyak K, Xia Y, Zweier JL, Kinzler KW and Vogelstein B: A model for p53-induced apoptosis. Nature 389: 300-305, 1997.

34. Baek KH, Bhang D, Zaslavsky A, Wang LC, Vachani A, Kim CF, Albelda SM, Evan GI and Ryeom S: Thrombospondin-1 mediates oncogenic Ras-induced senescence in premalignant lung tumors. J Clin Invest 123: 4375-4389, 2013.

35. Muller S, Filippakopoulos P and Knapp S: Bromodomains as therapeutic targets. Expert Rev Mol Med 13: e29, 2011.

36. Mazur G, Jaskuła E, Kryczek I, Dłubek D, Butrym A, Wróbel T, Lange A and Kuliczkowski K: Proinflammatory chemokine gene expression influences survival of patients with non-Hodgkin's lymphoma. Folia Histochem Cytobiol 49: 240-247, 2011.

37. Ouaguia L, Mrizak D, Renaud S, Moralès O and Delhem N: Control of the inflammatory response mechanisms mediated by natural and induced regulatory T-cells in HCV-, HTLV-1-, and EBV-associated cancers. Mediators Inflamm 2014: 564296, 2014.

38. Hinz M, Lemke P, Anagnostopoulos I, Hacker C, Krappmann D, Mathas S, Dörken B, Zenke M, Stein H and Scheidereit C: Nuclear factor kappaB-dependent gene expression profiling of Hodgkin's disease tumor cells, pathogenetic significance, and link to constitutive signal transducer and activator of transcription 5a activity. J Exp Med 196: 605-617, 2002.

39. Abbas T and Dutta A: p21 in cancer: Intricate networks and multiple activities. Nat Rev Cancer 9: 400-414, 2009.

40. Brown R and Plumb JA: Demethylation of DNA by decitabine in cancer chemotherapy. Expert Rev Anticancer Ther 4: 501-510, 2004.

41. Cruz CR, Gerdemann U, Leen AM, Shafer JA, Ku S, Tzou B, Horton TM, Sheehan A, Copeland A, Younes A, et al: Improving T-cell therapy for relapsed EBV-negative Hodgkin lymphoma by targeting upregulated MAGE-A4. Clin Cancer Res 17: 7058-7066, 2011.

42. Stewart ML, Tamayo P, Wilson AJ, Wang S, Chang YM, Kim JW, Khabele D, Shamji AF and Schreiber SL: KRAS genomic status predicts the sensitivity of ovarian cancer cells to decitabine. Cancer Res 75: 2897-2906, 2015.

43. Nishioka C, Ikezoe T, Yang J, Komatsu N, Koeffler HP and Yokoyama A: Blockade of MEK signaling potentiates 5-Aza-2'-deoxycytidine-induced apoptosis and upregulation of p21(waf1) in acute myelogenous leukemia cells. Int J Cancer 125: 1168-1176, 2009.

44. Guan H, Mi B, Li Y, Wu W, Tan P, Fang Z, Li J, Zhang Y and Li F: Decitabine represses osteoclastogenesis through inhibition of RANK and NF-κB. Cell Signal 27: 969-977, 2015.

45. Stevenson WS, Best OG, Przybylla A, Chen Q, Singh N, Koleth M, Pierce S, Kennedy T, Tong W, Kuang SQ, et al: DNA methylation of membrane-bound tyrosine phosphatase genes in acute lymphoblastic leukaemia. Leukemia 28: 787-793, 2014.

46. Lin JC, Wu YY, Wu JY, Lin TC, Wu CT, Chang YL, Jou YS, Hong TM and Yang PC: TROP2 is epigenetically inactivated and modulates IGF-1R signalling in lung adenocarcinoma. EMBO Mol Med 4: 472-485, 2012.

47. Han Y, Amin HM, Frantz C, Franko B, Lee J, Lin Q and Lai R: Restoration of shp1 expression by 5-AZA-2'-deoxycytidine is associated with downregulation of JAK3/STAT3 signaling in ALK-positive anaplastic large cell lymphoma. Leukemia 20: 1602-1609, 2006.

48. Galm O, Yoshikawa H, Esteller M, Osieka R and Herman JG: SOCS-1, a negative regulator of cytokine signaling, is frequently silenced by methylation in multiple myeloma. Blood 101: 2784-2788, 2003.

49. Laurenzana A, Petruccelli LA, Pettersson F, Figueroa ME, Melnick A, Baldwin AS, Paoletti F and Miller WH Jr: Inhibition of DNA methyltransferase activates tumor necrosis factor alpha-induced monocytic differentiation in acute myeloid leukemia cells. Cancer Res 69: 55-64, 2009.

50. Takebayashi S, Nakao M, Fujita N, Sado T, Tanaka M, Taguchi H and Okumura K: 5-Aza-2'-deoxycytidine induces histone hyperacetylation of mouse centromeric heterochromatin by a mechanism independent of DNA demethylation. Biochem Biophys Res Commun 288: 921-926, 2001.
51. Plumb JA, Strathdee G, Sludden J, Kaye SB and Brown R: Reversal of drug resistance in human tumor xenografts by 2'-deoxy-5-azacytidine-induced demethylation of the hMLH1 gene promoter. Cancer Res 60: 6039-6044, 2000.
52. Lou YF, Zou ZZ, Chen PJ, Huang GB, Li B, Zheng DQ, Yu XR and Luo XY: Combination of gefitinib and DNA methylation inhibitor decitabine exerts synergistic anti-cancer activity in colon cancer cells. PLoS One 9: e97719, 2014.
53. Hao Y, Chapuy B, Monti S, Sun HH, Rodig SJ and Shipp MA: Selective JAK2 inhibition specifically decreases Hodgkin lymphoma and mediastinal large B-cell lymphoma growth in vitro and in vivo. Clin Cancer Res 20: 2674-2683, 2014.
54. Jost PJ and Ruland J: Aberrant NF-kappaB signaling in lymphoma: Mechanisms, consequences, and therapeutic implications. Blood 109: 2700-2707, 2007.
55. Blum KA, Johnson JL, Niedzwiecki D, Canellos GP, Cheson BD and Bartlett NL: Single agent bortezomib in the treatment of relapsed and refractory Hodgkin lymphoma: Cancer and leukemia Group B protocol 50206. Leuk Lymphoma 48: 1313-1319, 2007.
56. Boucher MJ, Morisset J, Vachon PH, Reed JC, Lainé J and Rivard N: MEK/ERK signaling pathway regulates the expression of Bcl-2, Bcl-X(L), and Mcl-1 and promotes survival of human pancreatic cancer cells. J Cell Biochem 79: 355-369, 2000.
57. Chapuy B, McKeown MR, Lin CY, Monti S, Roemer MG, Qi J, Rahl PB, Sun HH, Yeda KT, Doench JG, *et al*: Discovery and characterization of super-enhancer-associated dependencies in diffuse large B cell lymphoma. Cancer Cell 24: 777-790, 2013.
58. Godley LA and Le Beau MM: The histone code and treatments for acute myeloid leukemia. N Engl J Med 366: 960-961, 2012.
59. Malik P and Cashen AF: Decitabine in the treatment of acute myeloid leukemia in elderly patients. Cancer Manag Res 6: 53-61, 2014.